A Link functions for different types of observations

In this paper, for decoder, we first develop GPFA, which is a shallow topic relational model (RTM) equipped with analytic conditional posteriors, and further extend it to GPGBN, a hierarchical (deep) generalization. For brevity, in the main manuscript, we only give a detailed discussion on the binary type of adjacency matrix $\mathbf{A}$ and a short introduction on how to build other types of $\mathbf{A}$. Thus, in this section, we will provide more detailed discussion on the continuous nonnegative and count-valued types of $\mathbf{A}$, which are also usually used in practice besides the binary type. Considering the likelihood of $\mathbf{A}$ is similar in GPFA and GPGBN, in the following, we take the observed adjacency matrix $\mathbf{A}$ in GPFA as an example to discuss. For completeness, we first discuss the binary $\mathbf{A}$ and then extend it to the continuous nonnegative and count-valued types.

Binary adjacency matrix: If the edge a_{ij} is binary to model whether two documents are associated, we can use a Bernoulli-Poisson (BerPo) link [11] expressed as

$$a_{ij} = 1(m_{ij} > 0), m_{ij} \sim \text{Pois}(\sum\nolimits_{k=1}^{K_1} u_k \theta_{ik} \theta_{jk}) \tag{10}$$

where $a_{ij} = 1$ if $m_{ij} \geq 1$ and $a_{ij} = 0$ if $m_{ij} = 0$. After m_{ij} is marginalized out, we can obtain a Bernoulli random variable as $a_{ij} \sim \text{Bern}(1 - \exp(-\sum_{k=1}^{K_1} u_k \theta_{ik} \theta_{jk}))$. The conditional posterior of the latent count m_{ij} can be expressed as

$$(m_{ij} \,|\, a_{ij}, \boldsymbol{u}, \boldsymbol{\theta_i}, \boldsymbol{\theta_i}) \sim a_{ij} \cdot \text{Pois}_{+}(\sum\nolimits_{k=1}^{K_1} u_k \theta_{ik} \theta_{jk}), \tag{11}$$

which can be simulated with a rejection sampler as described in Zhou et al. [11].

Continuous nonnegative adjacency matrix: If the edge a_{ij} is a continuous nonnegative value, like the cosine similarity between two documents, we can use gamma-Poisson link [20] expressed as

$$a_{ij} \sim \text{Gam}(m_{ij}, 1/c), m_{ij} \sim \text{Pois}(\sum\nolimits_{k=1}^{K_1} u_k \theta_{ik} \theta_{jk}) \tag{12}$$

whose distribution has a point mass at $a_{ij} = 0$ and is continue for $a_{ij} > 0$. Further the latent count $m_{ij} = 0$ if and only if $a_{ij} = 0$, and m_{ij} is a positive integer drawn from a truncated Bessel distribution if $a_{ij} > 0$.

Count-valued adjacency matrix: If the edge a_{ij} is a count value, such as indicating the frequency of citation, we can directly factor the discrete value a_{ij} under poisson likelihood as

$$a_{ij} \sim \text{Pois}(\sum\nolimits_{k=1}^{K_1} u_k \theta_{ik} \theta_{jk}) \tag{13}$$

To a conclusion, our models can be generalized to different types of networks with nodes and edges expressed by count, binary, or positive values via making full use of different link functions.

B Derivation for GPGBN

Here we describe the detailed derivation for graph Poisson gamma belief network (GPGBN) with T hidden layers, expressed as

$$\boldsymbol{x}_j^{(1)} \sim \text{Pois}(\boldsymbol{\Phi}^{(1)} \boldsymbol{\theta}_j^{(1)}), \left\{\boldsymbol{\theta}_j^{(t)} \sim \text{Gam}(\boldsymbol{\Phi}^{(t+1)} \boldsymbol{\theta}_j^{(t+1)}, 1/c_j^{(t+1)})\right\}_{t=1}^{T-1}, \boldsymbol{\theta}_j^{(T)} \sim \text{Gam}(\boldsymbol{\gamma}, 1/c_j^{(T+1)}),$$

$$a_{ij} = 1(\delta_{ij} > 1), \quad \delta_{ij} = \sum\nolimits_{t=1}^{T} m_{ij}^{(t)}, \quad \left\{m_{ij}^{(t)} \sim \text{Pois}(\sum\nolimits_{k=1}^{K_t} u_k^{(t)} \theta_{ik}^{(t)} \theta_{jk}^{(t)})\right\}_{t=1}^{T}, \tag{14}$$

B.1 Property

During the inference procedure, we adopt the variable augmentation and marginalization techniques of PGBN [20], exploiting the following properties of the Poisson, gamma, and related distributions:

Property 1 (P1): If $x_{\cdot} = \sum\limits_{n=1}^{N} x_n$, where $x_n \sim \text{Poisson}\,(\theta_n)$ are independent Poisson-distributed random variables, then we have $(x_1, \ldots, x_N) \sim \text{Multinomial}\left(x, \frac{\theta_1}{\sum_{n=1}^{N} \theta_n}, \ldots, \frac{\theta_N}{\sum_{n=1}^{N} \theta_n}\right)$ and $x_{\cdot} \sim \text{Poisson}\left(\sum_{n=1}^{N} \theta_n\right)$.

Property 2 (P2): If $x \sim \mathrm{Poisson}(c\theta)$, where c is a constant and $\theta \sim \mathrm{Gam}(a, 1/b)$, then we can marginalize out θ and obtain $x \sim \mathrm{NB}\left(a, \frac{c}{b+c}\right)$, satisfying a negative binomial (NB) distribution.

Property 3 (P3): If $x \sim \mathrm{NB}(a, p)$ and $l \sim \mathrm{CRT}(x, a)$ is a Chinese restaurant table-distributed random variable, then x and l are equivalently jointly distributed as $x \sim \mathrm{SumLog}(l, p)$ and $l \sim \mathrm{Poisson}(-\ln(1-p)a)$ [54].

B.2 Gibbs sampling

Gibbs sampling is a typical training algorithm for Bayesian models [12, 54, 20], and is applicable when there exist local conjugacies for latent variables, whose conditional distributions will then become tractable and simple to sample from, even though the posterior of the joint distribution of these variables is often intractable. Consistent to these aforementioned Bayesian models [12, 54, 20, 55], the proposed GPGBN provides analytic posteriors for all latent variables and the Gibbs sampling can be naturally applied, which have been proven efficient and can be further accelerated with GPU [43].

Making full use of these properties, we can obtain the following Poisson likelihoods for each hidden layer of GPGBN, formulated as:

$$x_{k_{t-1}j}^{(t)} \sim \text{Pois}(-\ln(1-p_j^{(t)}) \textstyle\sum_{k=1}^{K_t} \phi_{k_{t-1}k}^{(t)} \theta_{jk}^{(t)}), \tag{15}$$

$$m_{ij}^{(t)} \sim \text{Pois}(\textstyle\sum_{k=1}^{K_t} u_k^{(t)} \theta_{ik}^{(t)} \theta_{jk}^{(t)}), \tag{16}$$

Zhou2015Negative where the augmented node feature vector $\boldsymbol{x}_j^{(t)} \in \mathbb{R}_+^{K_{t-1}}$ and adjacency matrix $\boldsymbol{M}^{(t)} \in \mathbb{Z}^{N \times N}$ can be regarded as the specific observations at layer t. Thus, for each hidden layer of GPGBN, the analytic conditional posteriors for model parameters can be formulated as follows:

Sampling loading factor matirx $\boldsymbol{\Phi}^{(t)}$: Utilizing the simplex constraint on each column of $\boldsymbol{\Phi}^{(t)} \in \mathbb{R}_+^{K_{t-1} \times K_t}$, we can marginalize out $\boldsymbol{\theta}_j$ in (15) and have

$$(x_{1jk_t}^{(t)}, ..., x_{K_{t-1}jk_t}^{(t)} | x_{\cdot jk_t}^{(t)}) \sim \text{Multi}(x_{\cdot jk_t}^{(t)} \mid \boldsymbol{\phi}_{k_t}^{(t)}). \tag{17}$$

Therefore, via the Dirichlet-multinomial conjugacy, the posterior of $\boldsymbol{\phi}_{k_t}^{(t)}$ can be formulated as

$$(\boldsymbol{\phi}_{k_t}^{(t)} \mid -) \sim \text{Dir}(x_{1\cdot k_t}^{(t)} + \eta^{(t)}, ..., x_{K_{t-1}\cdot k_t}^{(t)} + \eta^{(t)}). \tag{18}$$

Sampling topic proportions $\boldsymbol{\theta}_j^{(t)}$: Benefit from jointly modeling node features and link structure under poisson likelihood, we have

$$(\theta_{jk_t}^{(t)} \mid -) \sim \text{Gam}\big(x_{\cdot jk_t}^{(t)} + \boldsymbol{\phi}_{k_t:}^{(t+1)} \boldsymbol{\theta}_j^{(t+1)} + \sum_{i \neq j} m_{ijk_t}^{(t)}, [-\ln(1-p_j^{(t)}) + c_j^{(t+1)} + u_{k_t}^{(t)} \sum_{i \neq j} \theta_{ik_t}^{(t)}]^{-1}\big). \tag{19}$$

where $x_{\cdot jk_t}^{(t)}$ and $m_{ijk_t}^{(t)}$ are latent count variables that are independently sampled from the corresponding node feature and relative edges at layer t, respectively.

Sampling scale parameter $c_j^{(t)}$ and $p_j^{(t)}$: To construct a hierarchical generative model, we introduce $c_j^{(t)} \sim \text{Gam}(e_0, 1/f_0)$ and the corresponding posterior of $c_j^{(t)}$ can be formulated as

$$(c_j^{(t)} \mid -) \sim \text{Gam}(\theta_{j\cdot}^{(t)} + e_0, 1/[f_0 + \theta_{j\cdot}^{(t-1)}]). \tag{20}$$

Referring the Lemma **1** of 20, $\{p_j^{(t)}\}_{t \geq 2}$ can be calculated with

$$p_j^{(t+1)} := -\ln(1-p_j^{(t)})/[c_j^{(t+1)} - \ln(1-p_j^{(t)})], \tag{21}$$

specifically defining $p_j^{(1)} := 1 - e^{-1}$.

Sampling $\boldsymbol{u}^{(t)}$: With the prior $u_{k_t}^{(t)} \sim \text{Gam}(\alpha_0, 1/\beta_0)$, via the gamma-Poisson conjugacy, we have

$$(u_{k_t}^{(t)} \mid -) \sim \text{Gam}(\textstyle\prod_{i=1}^{N} \prod_{j=1}^{i-1} m_{ijk_t}^{(t)} + \alpha_0, [\beta_0 + \prod_{i=1}^{N} \prod_{j=1}^{i-1} \theta_{ik_t}^{(t)} \theta_{jk_t}^{(t)}]^{-1}). \tag{22}$$

B.3 Time complexity analysis

Compared to the basic PGBN, the additional time cost for GPGBN is mainly in the procedure of graph augmentation, which can be formulated as

$$(m_{ij}^{(1)}, ..., m_{ij}^{(T)} \,|\, m_{ij}) \sim \text{Multi}(m_{ij}; \frac{\sum_{k_1=1}^{K_1} u_{k_t}^{(t)} \theta_{ik_1}^{(t)} \theta_{jk_1}^{(t)}}{\sum_{t=1}^{T} \sum_{k_t=1}^{K_t} u_{k_t}^{(t)} \theta_{ik_t}^{(t)} \theta_{jk_t}^{(t)}}, ..., \frac{\sum_{k_T=1}^{K_T} u_{k_T}^{(t)} \theta_{ik_T}^{(t)} \theta_{jk_T}^{(t)}}{\sum_{t=1}^{T} \sum_{k_t=1}^{K_t} u_{k_t}^{(t)} \theta_{ik_t}^{(t)} \theta_{jk_t}^{(t)}}), \tag{23}$$

$$(m_{ij1}^{(t)}, ..., m_{ijK_t}^{(t)} \,|\, m_{ij}^{(t)}) \sim \text{Multi}(m_{ij}^{(t)}; \frac{u_1^{(t)} \theta_{i1}^{(t)} \theta_{j1}^{(t)}}{\sum_{k_t=1}^{K_t} u_{k_t}^{(t)} \theta_{ik_t}^{(t)} \theta_{jk_t}^{(t)}}, ..., \frac{u_{K_t}^{(t)} \theta_{iK_t}^{(t)} \theta_{jK_t}^{(t)}}{\sum_{k_t=1}^{K_t} u_{k_t}^{(t)} \theta_{ik_t}^{(t)} \theta_{jk_t}^{(t)}}) \tag{24}$$

where the former indicates the multi-layer augmentation from m_{ij} and the latter denotes the augmentation at layer t. Here we note that there is no need to augment the whole adjacency matrix $\mathbf{A}$, but only the positive elements (edges) $\{a_{ij} > 0\}_{i=1,j=1}^{N,N}$ in $\mathbf{A}$. Thus the computational benefit is significant since the computational complexity is approximately linear to the number of $\{a_{ij} > 0\}_{i=1,j=1}^{N,N}$, denoted as S_a, in the observed adjacency matrix $\mathbf{A}$. Compared to directly handling with the whole matrix like traditional RTMs [14], this benefit is especially pertinent in many real-world network data where S_a is significantly smaller than N^2. Moreover, the augmentation operations for node features $\mathbf{X}$ or link structure $\mathbf{A}$ can be both processed with parallel Gibbs sampling [43], which can be further accelerated with GPU.

C Hybrid SGMCMC/VAE inference for WGAE & WGCAE

C.1 Stochastic gradient MCMC

Although the Gibbs sampler provided in Appendix B can be further accelerated with GPU, there is still a requirement for the GPGBN to preprocess all documents in each iteration and hence has limited scalability. For scalable inference, we consider to update global parameter $\mathbf{\Phi}^{(t)}$ by generalizing TLASGR-MCMC [46, 45], a SGMCMC algorithm that has been applied for the scalable inference for discrete latent variable models (LVMs) [56, 57]. More specifically, TLASGR-MCMC adopts an elegant simplex constraint and increases the sampling efficiency via the use of the Fisher information matrix (FIM), with adaptive step-sizes for the topics of different layers, which can be naturally extended to our model. The efficient TLASGR-MCMC update of $\boldsymbol{\phi}_k^{(t)}$ in GPGBN can be described as

$$\boldsymbol{\phi}_k^{(t)new} = \left\{ \boldsymbol{\phi}_k^{(t)} + \tfrac{\varepsilon_i^{(t)}}{\boldsymbol{M}_k^{(t)}} [(\rho \widetilde{\boldsymbol{x}}_{:k\cdot}^{(t)} + \boldsymbol{\eta}^{(t)}) - (\rho \widetilde{\boldsymbol{x}}_{\cdot k\cdot}^{(t)} + \boldsymbol{\eta}^{(t)} K_{t-1}) \boldsymbol{\phi}_k^{(t)}] + N\big(0, \tfrac{2\varepsilon_i^{(t)}}{\boldsymbol{M}_k^{(t)}} \text{diag}(\boldsymbol{\phi}_k^{(t)})\big) \right\}_{\angle}, \tag{25}$$

where i denotes the number of mini-batches processed so far; the symbol $\cdot$ in the subscript denotes summing over the data in a mini-batch; and the definitions of ρ, $\varepsilon_i^{(t)}$, $\boldsymbol{M}_k^{(t)}$ and $\{\cdot\}_{\angle}$ are analogous to these in [46] and omitted here for brevity.

C.2 Hybrid SGMCMC/VAE inference

Combining TLASGR-MCMC and the Weibull upward-downward variational inference network as described in Section 4.1, we can construct a hybrid stochastic-gradient MCMC/autoencoding variational inference for GPGBN. In detail, in each iteration, we adopt TLASGR-MCMC [46] to update $\{\mathbf{\Phi}^{(t)}\}_{t=1}^{T}$ and the standard Adam [58] to optimize $\{\mathbf{W}_e, \{u_k^{(t)}\}_{k=1,t=1}^{K_t,T}\}$ via maximizing the loss function formulated as

$$L = \sum_{j=1}^{N} \mathbb{E}\left[\ln p(\boldsymbol{x}_j | \mathbf{\Phi}^{(1)}, \boldsymbol{\theta}_j^{(1)})\right] + \beta \mathbb{E}\left[\ln p(\boldsymbol{A} | \{\mathbf{\Theta}^{(t)}\}_{t=1}^{T})\right] - \sum_{j=1}^{N} \sum_{t=1}^{T} \mathbb{E}\left[\ln \frac{q(\boldsymbol{\theta}_j^{(t)} | -)}{p(\boldsymbol{\theta}_j^{(t)} | \mathbf{\Phi}^{(t+1)}, \boldsymbol{\theta}_j^{(t+1)})}\right]. \tag{26}$$

For more efficient computation, the proposed hybrid stochastic-gradient MCMC/autoencoding variational inference algorithm in Algorithm 1, which is implemented in TensorFlow [47], combined with pyCUDA [48].

Algorithm 1 Hybrid stochastic-gradient MCMC and variational autoencoder inference for WGAE and WGCAE

```
Set mini-batch size $m \le N$ and number of layer $T$;
Initialize parameters $\{\{\mathbf{\Phi}^{(t)}\}_{t=1}^{T}, \{u_k^{(t)}\}_{k=1,t=1}^{K_t,T}, \mathbf{W}_e\}$;
for $iter = 1, 2, \cdots$ do
    For all documents $\mathbf{X} \in \mathbb{Z}^{K_0 \times N}$ and $\mathbf{A} \in \{0,1\}^{N \times N}$ draw random noise $\boldsymbol{\varepsilon} = \{\boldsymbol{\varepsilon}_j^{(t)}\}_{j=1,t=1}^{N,T}$;
    Calculate $\nabla_{\mathbf{W}_e, \boldsymbol{u}} L(\mathbf{W}_e, \boldsymbol{u}; \mathbf{X}, \mathbf{A}, \boldsymbol{\varepsilon})$ according to (25) and update $\{\mathbf{W}_e, \boldsymbol{u} = \{u_k^{(t)}\}_{k=1,t=1}^{K_t,T}\}$;
    Randomly select a mini-batch of $m$ documents to form a subset $\mathbf{X}_s = \{\boldsymbol{x}_j\}_{j=1}^{m}$;
    Sample corresponding topic proportions $\{\boldsymbol{\theta}_j^{(t)}\}_{j=1,t=1}^{m,T}$ to update $\{\mathbf{\Phi}^{(t)}\}_{t=1}^{T}$ according to (6);
end for
```

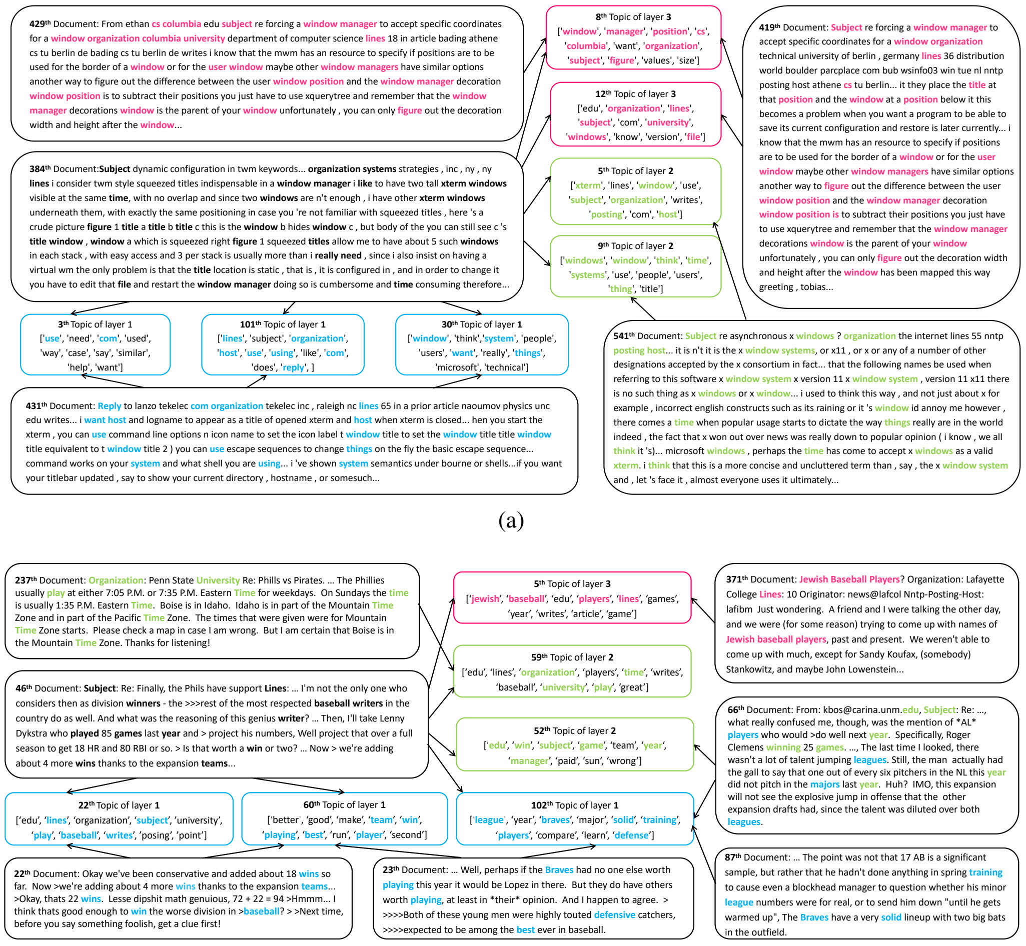

8th Topic of layer 3
['window', 'manager', 'position', 'cs', 'columbia', 'want', 'organization', 'subject', 'figure', 'values', 'size']
12th Topic of layer 3
['edu', 'organization', 'lines', 'subject', 'com', 'university', 'windows', 'know', 'version', 'file']
5th Topic of layer 2
['xterm', 'lines', 'window', 'use', 'subject', 'organization', 'writes', 'posting', 'com', 'host']
9th Topic of layer 2
['windows', 'window', 'think', 'time', 'systems', 'use', 'people', 'users', 'thing', 'title']
3th Topic of layer 1
['use', 'need', 'com', 'used', 'way', 'case', 'say', 'similar', 'help', 'want']
101th Topic of layer 1
['lines', 'subject', 'organization', 'host', 'use', 'using', 'like', 'com', 'does', 'reply',]
30th Topic of layer 1
['window', 'think','system', 'people', 'users', 'want', 'really', 'things', 'microsoft', 'technical']
(a)
5th Topic of layer 3
['jewish', 'baseball', 'edu', 'players', 'lines', 'games', 'year', 'writes', 'article', 'game']
59th Topic of layer 2
['edu', 'lines', 'organization', 'players', 'time', 'writes', 'baseball', 'university', 'play', 'great']
52th Topic of layer 2
['edu', 'win', 'subject', 'game', 'team', 'year', 'manager', 'paid', 'sun', 'wrong']
22th Topic of layer 1
['edu', 'lines', 'organization', 'subject', 'university', 'play', 'baseball', 'writes', 'posing', 'point']
60th Topic of layer 1
['better', 'good', 'make', 'team', 'win', 'playing', 'best', 'run', 'player', 'second']
102th Topic of layer 1
['league', 'year', 'braves', 'major', 'solid', 'training', 'players', 'compare', 'learn', 'defense']
(b)

429th Document: From ethan cs columbia edu subject re forcing a window manager to accept specific coordinates for a window organization columbia university department of computer science lines 18 in article bading athene cs tu berlin de bading cs tu berlin de writes i know that the mwm has an resource to specify if positions are to be used for the border of a window or for the user window maybe other window managers have similar options another way to figure out the difference between the user window position and the window manager decoration window position is to subtract their positions you just have to use xquerytree and remember that the window manager decorations window is the parent of your window unfortunately , you can only figure out the decoration width and height after the window...

384th Document:**Subject** dynamic configuration in twm keywords... **organization systems** strategies , inc , ny , ny **lines** i consider twm style squeezed titles indispensable in a **window manager** i **like** to have two tall **xterm windows** visible at the same **time**, with no overlap and since two **windows** are n't enough , i have other **xterm windows** underneath them, with exactly the same positioning in case you 're not familiar with squeezed titles , here 's a crude picture **figure** 1 **title** a **title** b **title** c this is the **window** b hides **window** c , but body of the you can still see c 's **title window** , **window** a which is squeezed right **figure** 1 squeezed **titles** allow me to have about 5 such **windows** in each stack , with easy access and 3 per stack is usually more than i **really need** , since i also insist on having a virtual wm the only problem is that the **title** location is static , that is , it is configured in , and in order to change it you have to edit that **file** and restart the **window manager** doing so is cumbersome and **time** consuming therefore...

419th Document: Subject re forcing a window manager to accept specific coordinates for a window organization technical university of berlin , germany lines 36 distribution world boulder parcplace com bub wsinfo03 win tue nl nntp posting host athene cs tu berlin... it they place the title at that position and the window at a position below it this becomes a problem when you want a program to be able to save its current configuration and restore is later currently... i know that the mwm has an resource to specify if positions are to be used for the border of a window or for the user window maybe other window managers have similar options another way to figure out the difference between the user window position and the window manager decoration window position is to subtract their positions you just have to use xquerytree and remember that the window manager decorations window is the parent of your window unfortunately , you can only figure out the decoration width and height after the window has been mapped this way greeting , tobias...

431th Document: Reply to lanzo tekelec com organization tekelec inc , raleigh nc lines 65 in a prior article naoumov physics unc edu writes... i want host and logname to appear as a title of opened xterm and host when xterm is closed... hen you start the xterm , you can use command line options n icon name to set the icon label t window title to set the window title title window title equivalent to t window title 2) you can use escape sequences to change things on the fly the basic escape sequence... command works on your system and what shell you are using... i 've shown system semantics under bourne or shells...if you want your titlebar updated , say to show your current directory , hostname , or somesuch...

541th Document: Subject re asynchronous x windows ? organization the internet lines 55 nntp posting host... it is n't it is the x window systems, or x11 , or x or any of a number of other designations accepted by the x consortium in fact... that the following names be used when referring to this software x window system x version 11 x window system , version 11 x11 there is no such thing as x windows or x window... i used to think this way , and not just about x for example , incorrect english constructs such as its raining or it 's window id annoy me however , there comes a time when popular usage starts to dictate the way things really are in the world indeed , the fact that x won out over news was really down to popular opinion (i know , we all think it 's)... microsoft windows , perhaps the time has come to accept x windows as a valid xterm. i think that this is a more concise and uncluttered term than , say , the x window system and , let 's face it , almost everyone uses it ultimately...

237th Document: Organization: Penn State University Re: Phills vs Pirates. … The Phillies usually play at either 7:05 P.M. or 7:35 P.M. Eastern Time for weekdays. On Sundays the time is usually 1:35 P.M. Eastern Time. Boise is in Idaho. Idaho is in part of the Mountain Time Zone and in part of the Pacific Time Zone. The times that were given were for Mountain Time Zone starts. Please check a map in case I am wrong. But I am certain that Boise is in the Mountain Time Zone. Thanks for listening!

46th Document: **Subject**: Re: Finally, the Phils have support **Lines**: … I'm not the only one who considers then as division **winners** - the >>>rest of the most respected **baseball writers** in the country do as well. And what was the reasoning of this genius **writer**? … Then, I'll take Lenny Dykstra who **played** 85 **games** last **year** and > project his numbers, Well project that over a full season to get 18 HR and 80 RBI or so. > Is that worth a **win** or two? … Now > we're adding about 4 more **wins** thanks to the expansion **teams**...

371th Document: Jewish Baseball Players? Organization: Lafayette College Lines: 10 Originator: news@lafcol Nntp-Posting-Host: lafibm Just wondering. A friend and I were talking the other day, and we were (for some reason) trying to come up with names of Jewish baseball players, past and present. We weren't able to come up with much, except for Sandy Koufax, (somebody) Stankowitz, and maybe John Lowenstein...

66th Document: From: kbos@carina.unm.edu, Subject: Re: …, what really confused me, though, was the mention of *AL* players who would >do well next year. Specifically, Roger Clemens winning 25 games. …, The last time I looked, there wasn't a lot of talent jumping leagues. Still, the man actually had the gall to say that one out of every six pitchers in the NL this year did not pitch in the majors last year. Huh? IMO, this expansion will not see the explosive jump in offense that the other expansion drafts had, since the talent was diluted over both leagues.

22th Document: Okay we've been conservative and added about 18 wins so far. Now >we're adding about 4 more wins thanks to the expansion teams... >Okay, thats 22 wins. Lesse dipshit math genuious, 72 + 22 = 94 >Hmmm... I think thats good enough to win the worse division in >baseball? > >Next time, before you say something foolish, get a clue first!

23th Document: … Well, perhaps if the Braves had no one else worth playing this year it would be Lopez in there. But they do have others worth playing, at least in *their* opinion. And I happen to agree. > >>>>Both of these young men were highly touted defensive catchers, >>>>expected to be among the best ever in baseball.

87th Document: … The point was not that 17 AB is a significant sample, but rather that he hadn't done anything in spring training to cause even a blockhead manager to question whether his minor league numbers were for real, or to send him down "until he gets warmed up", The Braves have a very solid lineup with two big bats in the outfield.

Figure 5: Visualization of document subnetworks learned by a 3-layer GPGBN on 20news dataset. The detailed visualization procedures are analogous to the description in Section 5.1.

D Visualizations of hierarchical semantic topics and relationships

D.1 Visualizations of subnetworks learned by GPGBN

To further investigate the interpretability of our models, we visualize more document subnetworks learned by a 3-layer GPGBN on 20news dataset, as shown in Fig. 5. More specifically, we select the 384th and 46th documents, whose contents focus on different semantic topics, as source nodes and the detailed visualization procedures are analogous to the description in Section 5.1.

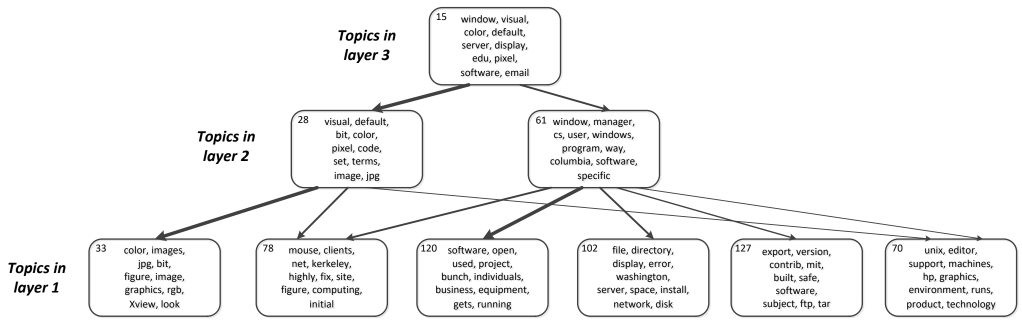
Topics in layer 3
15 window, visual, color, default, server, display, edu, pixel, software, email
Topics in layer 2
28 visual, default, bit, color, pixel, code, set, terms, image, jpg
61 window, manager, cs, user, windows, program, way, columbia, software, specific
Topics in layer 1
33 color, images, jpg, bit, figure, image, graphics, rgb, Xview, look
78 mouse, clients, net, kerkeley, highly, fix, site, figure, computing, initial
120 software, open, used, project, bunch, individuals, business, equipment, gets, running
102 file, directory, display, error, washington, server, space, install, network, disk
127 export, version, contrib, mit, built, safe, software, subject, ftp, tar
70 unix, editor, support, machines, hp, graphics, environment, runs, product, technology

(a)

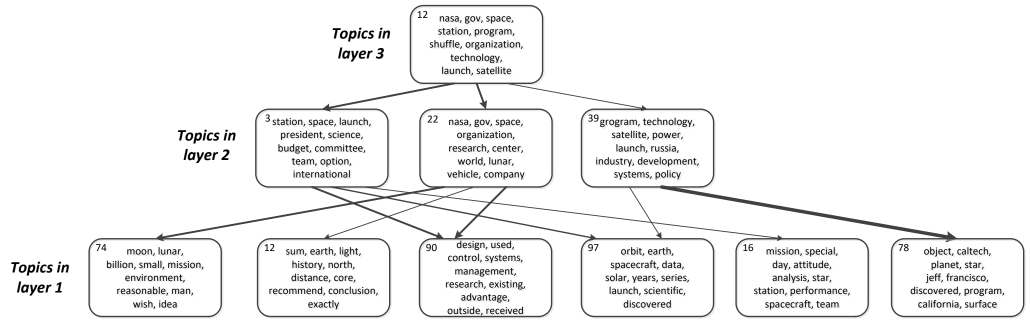
Topics in layer 3
12 nasa, gov, space, station, program, shuffle, organization, technology, launch, satellite
Topics in layer 2
3 station, space, launch, president, science, budget, committee, team, option, international
22 nasa, gov, space, organization, research, center, world, lunar, vehicle, company
39 grogram, technology, satellite, power, launch, russia, industry, development, systems, policy
Topics in layer 1
74 moon, lunar, billion, small, mission, environment, reasonable, man, wish, idea
12 sum, earth, light, history, north, distance, core, recommend, conclusion, exactly
90 design, used, control, systems, management, research, existing, advantage, outside, received
97 orbit, earth, spacecraft, data, solar, years, series, launch, scientific, discovered
16 mission, special, day, attitude, analysis, star, station, performance, spacecraft, team
78 object, caltech, planet, star, jeff, francisco, discovered, program, california, surface

(b)

Figure 6: Visualization of hierarchical topics learned by 3-layer GPGBNs on 20news dataset.

Table 3: Topic-coherence comprasion of GPGBN and PGBN on 20news dataset.

Topic layers	hardware	christian	guns	space	graphics
LDA [12]	0.530	0.561	0.491	0.538	0.564
PFA [54]	0.494	0.560	0.483	0.520	0.555
DPFA [19]	0.581	0.604	0.535	0.562	0.575
PGBN [20]	0.607	0.615	0.550	0.578	0.583
GPGBN	**0.638**	**0.641**	**0.602**	**0.623**	**0.613**

D.2 Visualizations of hierarchical semantic topics

Aiming at intuitively visualizing multi-layer semantics captured by GPGBN, we follow PGBN [20] to construct topic trees to visualize the GPGBN learned on 20news dataset. The 20news dataset in our experiments consists documents from 20 different news groups, with a pre-pruned vocabulary of size $K_0 = 2000$. Considering there is no observed adjacency matrix for 20News dataset, we first represent each document as a bag-of-word (BOW) vector to consider global semantics, and then construct the adjacency matrix via measuring the cosine similarity between documents. Setting the hyperparameters same as described in Appendix E, we construct 3-layer GPGBNs with same network structures of $[K_1, K_2, K_3] = [128, 64, 32]$ for different news groups, respectively, and train these GPGBNs with collapsed Gibbs sampling algorithms after 1000 iterations.

As shown in Fig. 6, for each tree, we pick a node at top layer and grow the tree downward by drawing a line from node k at layer t, the root or a leaf node of the tree, to node k' at layer $t-1$ for all k' in the set $\{k' : \mathbf{\Phi}^{(t)}_{k'k} > \tau_t / K_{t-1}\}$ and use τ_t to adjust the complexity of this tree. For each topic $\phi^{(t)}_k$, we exhibit top-10 word to represent the corresponding semantics and there is a clearly trend that the proposed GPGBN can capture hierarchical semantics with multiple semantic latent representations. More specifically, with the increasing of topic layers, the topic semantics vary from specific to general, due to the fact that higher topics are composed of the lower ones as introduced in Section 3.4.

To make a quantitative comparison between the topics learned GPGBN and other topic models, including LDA [12], PFA [54], DPFA [19] and PGBN [20], we adopt the topic coherence [59], which measures the semantic coherence in the most significant words (top words) of a topic, as the metric to measure the quality of the learned topics. More specifically, we construct various topic models for each news group of 20news dataset, and then evaluate topic coherence on the top hidden layers of the same size. From the results on different news groups shown in Table. 3, the words among the topics learned by GPGBN are more relevant (or co-occurrence) than those learned by other methods, benefiting from introducing the graph likelihood upon multi-layer document latent representations.

E Dataset and model setting

E.1 Dataset and preprocess

Six widely used datasets are considered in our experiment part, including Coil [5], TREC [43], and R8 [49] for node clustering; Cora, Citeseer and Pubmed [50] for link prediction and node classification. The detailed summary statistics of these benchmark datasets are listed in Table 4.

For node clustering, we follow the preprocess of GNMF [5], constructing a binary adjacency matrix via measuring the consine similarity between node features and then thresholding the matrix with

$$a_{ij} = \begin{cases} 1 & \text{if } \cos(\boldsymbol{x}_i, \boldsymbol{x}_j) \geq \tau \\ 0 & \text{if } \cos(\boldsymbol{x}_i, \boldsymbol{x}_j) < \tau, \end{cases} \tag{27}$$

where τ is a pre-set hyperparameter and a larger τ indicates a more sparse adjacency matrix.

For link prediction and node classification, the node features and adjacency matrix are provided by VGAE [23], and we directly follow the preprocess published in their code. To make a fair comparison, we adopt the same train/test/validate split as other methods. More specifically, for link prediction, we train the model on an incomplete version of the network data, with 5%/10% of the citation links used for validation/test and the validation set for node classification is fixed same as the other methods.

Table 4: Statistics of the datasets for various tasks.

Task	Dataset	Nodes	Edges	Features	Classes
node clustering	Coil	1,440	4,201	1,024	20
	TREC	5952	18,013	2000	8
	R8	7674	27,513	2000	8
link prediction or node classification	Cora	2,708	5,429	1,433	7
	Citeseer	3,327	4,732	3,703	6
	Pubmed	19,717	44,338	500	3

E.2 Model setting

Hyperparameter setting: To make an intuitive introduction for hyperparameter settings of our models, we list a tabular overview of parameters names, meanings and corresponding hyperparameter settings in Table 5. Here we note that the following hyperparameter settings are suitable for all our models including GPFA/GPGBN and WGAE/WGCAE.

Table 5: Hyperparameters settings.

Parameter Priors	Parameter means	Hyperparameters settings
$\boldsymbol{\phi}_{k_t}^{(t)} \sim \mathrm{Dir}(\eta^{(t)})$	The k_t topic at layer t	$\eta^{(t)} = 0.01$
$c_j^{(t)} \sim \mathrm{Gam}(e_0, 1/f_0)$	The scale parameter of $\boldsymbol{\theta}_j$	$e_0 = 1, f_0 = 1$
$u_{k_t}^{(t)} \sim \mathrm{Gam}(\alpha_0, 1/\beta_0)$	The importance weight of $\theta_{k_t j}^{(t)}$	$\alpha_0 = 1, \beta_0 = 1$

Network structure setting: We perform three WGAEs/WGCAEs with different stochastic layers, *i.e.*, $T \in \{1, 2, 3\}$, and set the network structure as $K_1 = K_2 = K_3 = C$, where C is set as the total number of classes for node clustering/classification as listed in Table 4, and 16 for link prediction following SIG-VAE [4]. The trade-off parameter β in (6) is decided based on the validation data for

Table 6: Comparisons on node classification performances.

Method	**Cora**	**Citeseer**	**Pubmed**
ManiReg [60]	59.5	60.1	70.7
SemiEmb [61]	59.0	59.6	71.1
LP [62]	68.0	45.3	63.0
DeepWalk [6]	67.2	43.2	65.3
ICA [63]	75.1	69.1	73.9
Planetoid [64]	75.7	64.7	77.2
GCN [24]	81.5	70.3	79.0
SIG-VAE [4]	79.7	70.4	**79.3**
GAT-16[4] [65]	<u>82.3</u>	71.9	78.7
GAT-64[4] [65]	**83.0**	**72.5**	79.0
WGCAE	82.0	<u>72.1</u>	<u>79.1</u>

various graph analysis tasks. For optimization, we adopt the standard Adam [58] with learning rate 0.001 to optimize the whole loss function in (6).

F Node classification task

Distinct from the pure probabilistic model GPFA/GPGBN having difficulty to plug in side information, the proposed WGAE/WGCAE are more flexible that can be extended for supervised learning, owing to the VAE-like structure. To make a full investigation for our models, we also perform node classification task with a single-layer WGCAE in this part. Given node labels $\{y_j\}_{j=1}^{N}$, we incorporate a categorical likelihood $p(y_j \mid \boldsymbol{\theta}_j)$ into (6), leading to a supervised model, and the corresponding supervised loss function can be formulated as

$$L_s = \sum_{j=1}^{N} \mathbb{E}\left[\ln p(y_j|\boldsymbol{\theta}_j)\right] + L. \tag{28}$$

To make a fair comparison, we set the hidden units of all methods to 16 following SIG-VAE[4] [4], and the compared results are listed in Table 6. From the node classification results, the proposed WGCAE exhibits strong generalization properties, achieving comparable results on Cora, Citeseer and Pubmed, despite not being trained specifically for node classification task. More specifically, the GCN-based WGCAE outperforms other GCN-based methods and even achieves higher performance than GAT under same network settings. We attribute the advantages of WGCAE to following reasons: i) similar to SIG-VAE, the reconstruction for edges and node features effectively alleviate overfitting, which is particularly serious in small datasets like Cora and Citeseer; ii) distinct from other methods providing discriminative dense node representations, the WGCAE introduces uncertainty and sparsity into latent representations with Weibull distribution, which is more suitable to approximate sparse and skewed document latent representations.

G Discussion about SIG-VAE and WGCAE

We clarify that SIG-VAE [4] and the proposed WGCAE focus on different aspects of improvements, although they are both built on VGAE [23]. SIG-VAE adopts a semi-implicit hierarchical construction, whose first layer is still limited by Gaussian, to support a more complex variational posterior. Moving beyond Gaussian distributions, the proposed WGCAE takes a different approach that uses a Weibull distribution to approximate sparse and skewed gamma distributed conditional posteriors. Moreover, we note that the semi-implicit technique [42] used by SIG-VAE can also be introduced to move WGCAE beyond its Weibull variational distribution, which we leave for future study.

For quantitative comparisons between SIG-VAE and WGCAE, although SIG-VAE outperforms WGCAE in two benchmarks for link prediction, it takes much heavier computation and memory

[4]Note the original GAT uses 64 hidden features (GAT-64), and we also report the results of GAT with 16 hidden features (GAT-16) to make a fair comparison.

Table 7: Comparisons on node clustering performances.

Method	**Cora**		**Citeseer**	
	ACC	NMI	ACC	NMI
VGAE [23]	59.2	0.43	51.5	0.20
SIG-VAE [4]	68.8	0.58	57.4	0.34
WGCAE	**74.6**	**0.62**	**66.5**	**0.41**

cost. More specifically, for SIG-VAE, if naively implemented, the memory cost is theoretically $(K + J)$ times larger than the most basic VGAE, where K and J represents the sampling numbers of SIVI [32] in each iteration. For example, SIG-VAE takes nearly 0.7G $(K = 1, J = 1)$, 4.4G $(K = 5, J = 10)$, and 10.6G $(K = 15, J = 20)$ RAM cost on Cora with 2708 nodes. Following this trend, a naively implemented SIG-VAE is estimated to take a normally unaffordable memory when setting $(K = 150, J = 2000)$. By contrast, a 3-layer WGCAE, which takes only 1.3G RAM, has achieved a comparable link prediction performance and outperformed SIG-VAE on both node clustering and classification tasks, showing the proposed WGCAE is more efficient than SIG-VAE. Further, benefiting from introducing node feature reconstruction, WGCAE significantly outperforms SIG-VAE in node clustering tasks, and we perform additional comparisons between WGCAE and the clustering results provided in the appendix of SIG-VAE [4], as shown in Table 7.